Power Laws and Similarity of Rayleigh-Taylor and Richtmyer-Meshkov Mixing Fronts at All Density Ratios

U. Alon,[1] J. Hecht,[1] D. Ofer,[1] and D. Shvarts[1,2]

[1]*Physics Department, Nuclear Research Centre Negev, P.O. Box 9001, Beer-Sheva 84190, Israel*

[2]*Laboratory for Laser Energetics, University of Rochester, 250 East River Road, Rochester, New York 14623-1299*

(Received 16 September 1994)

The nonlinear evolution of large structure in Rayleigh-Taylor and Richtmyer-Meshkov bubble and spike fronts is studied numerically and explained theoretically on the basis of single-mode and two-bubble interaction physics at Atwood numbers (A). Multimode Rayleigh-Taylor bubble (spike) fronts are found as $h_B = \alpha_B A g t^2$ [$h_s = \alpha_s(A) g t^2$] with $\alpha_B = 0.05$, while Richtmyer-Meshkov bubble (spike) fronts are found as $h_B = a_B t^{\theta_B}$ ($h_s = a_s t^{\theta_s(A)}$) with $\theta_B = 0.4$ at all A's. The dependence of these scaling laws and parameters on A and on initial conditions is explained.

PACS numbers: 47.20.–k, 52.35.Py

The Rayleigh-Taylor (RT) instability [1] that occurs when a fluid accelerates another fluid of higher density and the Richtmyer-Meshkov [2] (RM) instability that occurs when a shock wave passes an interface between two fluids are of extreme importance in achieving inertial confinement fusion [3] and in understanding astrophysical phenomena. Under these instabilities, small perturbations on the interface grow into bubbles of light fluid and spikes of heavy fluid. In the multimode RT instability, both the bubble and the spike fronts grow as gt^2, where g is the driving acceleration and exhibits a self-similar behavior with this scale [4,5]. In that case it is natural that gt^2 is the only dimensional length scale of the problem after the initial conditions have been forgotten. In contrast, the impulsive nature of the RM instability does not induce such a well-defined, self-similar law of fluid interpenetration. Many attempts to experimentally [6], theoretically [7], or numerically [8–10] derive a simple scaling law for the RM case did not result in a satisfactory theory that could predict the nonlinear evolution of the mixing zone. Recently, Alon *et al.* [11] applied a bubble competition model to study the time evolution of bubble fronts in both RT and RM, in the limit of Atwood number $A = 1$. The front was modeled by an array of bubbles (in 2D), rising with their single-mode velocity obtained from Layzer's potential flow model [12,13]. Bubbles overtake their smaller neighbors and form larger bubbles ("bubble merger") [2,14,15] at a rate ω that was calculated from an extended potential flow model of two-bubble competition [11,13]. The asymptotic behavior of the $A = 1$ RT bubble front was found to be $h_B = \alpha_B g t^2$, with $\alpha_B = 0.05$, in agreement with previous studies [4,5,15]. The $A = 1$ RM asymptotic bubble-front evolution was found to obey a new power law: $h_B = a_B t^{\theta_B}$ with $\theta_B = 0.4$, which was then confirmed by full 2D numerical simulations. As for the spike front, in the $A = 1$ RT case it is in free-fall [2], $h_s = \frac{1}{2} g t^2$, exhibiting the same time behavior as the bubble front, but with a different coefficient. In the RM case, the $A = 1$ spikes fall at a constant velocity. Thus, in contrast with RT, the $A = 1$ RM spike and bubble fronts exhibit different power laws, and the mixing-zone width cannot be described as a single power law of time. The main purpose of the present Letter is to address the question of the late time evolution of the RT and RM bubble and spike fronts at all A's. New RM scaling laws are derived and the familiar RT scaling laws are explained, based on the same fundamental mechanisms of single-mode evolution and two-bubble interaction. We thus begin by studying these two basic elements of the model and then consider the multimode case.

Single Mode Perturbations.—We now detail our results for the RM single-mode case; analogous results have been obtained for the RT case. We consider the instability of an interface between two inviscid fluids with (post-shock) densities ρ_1 and ρ_2. The Atwood number is $A = (\rho_1 - \rho_2)/(\rho_1 + \rho_2)$. A shock impinges on an interface perturbation of wavelength $\lambda = 2\pi/k$ and generates a velocity perturbation of amplitude u_0, as given by linear theory [1,9,16]. After a short time of order λ/U (U is the shock velocity), there is no further interaction with the shock [1,8,10,17,18]. An expansion of the flow equations to second order yields [18] $u(t) = u_0(1 \pm A k u_0 t)$ (the minus sign is for the bubble, the plus for the spike), showing that the bubble velocity begins to decrease. At late times, the $A = 1$ bubble attains an asymptotic velocity of $u_B = (3\pi)^{-1}\lambda/t$ [13,17]. The transition to this asymptotic stage occurs at a bubble amplitude of roughly $0.1\ \lambda$, as in the RT case [13]. In order to study the bubble and spike behavior, for various density ratios, we performed full-scale hydrodynamic simulation using LEEOR2D [5,19], a compressible ALE code with interface tracking. The initial condition used was single cosine-mode perturbations in velocity. The simulations were done in the incompressible limit (the sound velocity was much larger than the perturbation velocity). The bubble velocities found are shown in Fig. 1. At $A < 1$, the bubble velocity initially decays more slowly than at $A = 1$, in accordance with the second-order expansion. At late times all bubble velocities approach the same asymptotic form, $u_B = c_B \lambda/t$, where $c_B = (3\pi)^{-1} \approx 0.11$ for $A \gtrsim 0.5$ and rises to about

 0031-9007/95/74(4)/534(4)$06.00

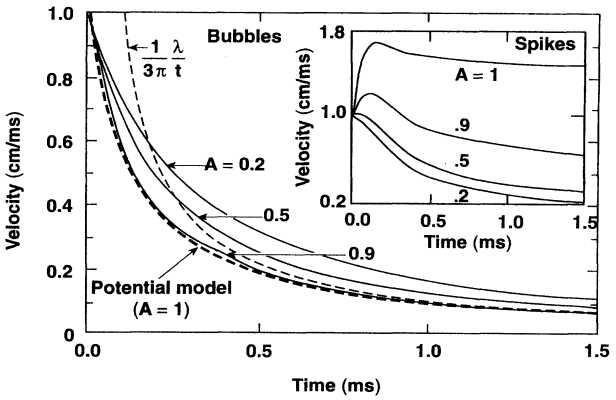

FIG. 1. Single-mode RM bubble velocities. We choose units typical of shock-tube experiments [6] $\lambda = 1$ cm and $u_0 = 1$ cm/ms. Note that in all RM results in this Letter (i) the initial velocities can be related to the initial amplitude of the interface perturbation a_0 and the interface jump velocity ΔU by Richtmyer's formula [1,16] $u_0 = 2\pi A \Delta U a_0/\lambda$, and (ii) units can be rescaled using $\{u \to su, \lambda \to s'\lambda, t \to (s'/s)t\}$. Also plotted are the potential flow model results [13] and the asymptotic velocity [13]. Inset: spike velocities.

$c_B \approx 0.15$ at low A's. The spike velocities are shown in Fig. 1 inset. The $A = 1$ spike initially accelerates, in accordance with the second-order expansion, and then saturates to a constant velocity [8,13]. At $A < 1$ the spike velocity also initially rises and then begins to decrease, asymptotically going as λ/t, due to the development of a rounded head that increases the drag of the light fluid. Analogously, in the RT case, the spike reaches a constant acceleration at $A = 1$ and a constant velocity at $A < 1$ [2]. Thus, the total mixing zone growth rate asymptotically goes as λ/t, in agreement with the analysis of the full-shock simulations of Ref. [20]. Some physical intuition for this behavior may be gained with a simplified model for the bubble. Schematically, Newton's equation for the heavy fluid above the bubble is $\rho_1 V \partial u/\partial t = -c_D \rho_1 u^2 S + c(\rho_1 - \rho_2) g V$, where V is the volume of fluid set in motion by the bubble [21]. The drag term [22,23] $F_{\text{drag}} \approx -c_D \rho_1 u^2 S$, where S is the bubble area [22], is equal to the change of momentum of the heavy fluid per unit time by the bubble obstruction. Thus, using $V/S \sim \lambda$, the RM bubble velocity ($g = 0$) is $u_B \sim \lambda/t$. The RT asymptotic single-mode bubble velocity is given by a balance of buoyancy and drag, leading to $u_B \sim \sqrt{2A/(1 + A) g\lambda}$ [23]. Similar arguments for the spikes, replacing ρ_1 by ρ_2 in the drag term, show that $u_s \sim 2A/(1 - A)\lambda/t$ in RM and $u_s \sim \sqrt{2A/(1 - A) g\lambda}$ in RT. These results are in agreement with our numerical simulations. Thus, the reason larger bubbles (and spikes) grow faster is that they have a smaller ratio of area to displaced fluid volume, and therefore less drag per unit mass. (Note that in the RT case, larger structures have less drag and equal buoyancy per unit mass.) This is the fundamental reason for the inverse cascade in both instabilities.

Two-Bubble Competition.—We performed simulations of two-bubble competition for both the RT and RM cases, for various A's. The initial velocity field in this case is a sum of two modes with wave numbers k and $2k$ and amplitudes u_1 and u_2. This perturbation corresponds, at early times, to two bubbles with velocities $u_1 \pm u_2$. The RT case was previously studied in Refs. [11–15,24]. We find that for both RT and RM cases, at early times, the two bubbles rise independently. Later, the large bubble expands and rises faster, while the slower bubble shrinks and is swept downstream into the spike of the surviving bubble. Asymptotically, a periodic array of spikes and bubbles of wavelength 2λ remains. The competition rate is the rate at which the large bubble's velocity increases from coexistence at a wavelength of about λ to saturation at wavelength 2λ. In the RT case, we find that the competition process takes longer for smaller Atwood numbers: The merger rate is $\omega(A) \simeq \omega(A = 1)\sqrt{A(1 + A)/2}$, where $\omega(A = 1)$ is the potential flow merger rate for $A = 1$ [11]. This can be explained by noting that during the overtake phase, the larger bubble accelerates at a nearly constant acceleration of $g_0 \sim 0.1Ag$, as was also found in previous studies [14], its velocity increases by $\Delta u \sim \sqrt{2A/(1 + A)}(\sqrt{2\lambda g} - \sqrt{\lambda g})$, and hence the merger rate is $\omega \sim g_0/\Delta u \sim \sqrt{A(1 + A)/2}\, g/\lambda$. In contrast, the RM merger rate is found to be very insensitive to the Atwood number and is in good agreement with the $A = 1$ bubble-competition potential flow model [13].

Multimode Fronts.—Multimode (or random) fronts grow from initial perturbations composed of many short-wavelength modes. The merger model [11,25] predicts that both the RM and RT front dynamics flow to a scale-invariant regime, similar to that derived in Ref. [15] for the RT case, where the bubble-size distribution scales with the average bubble wavelength. The average wavelength is predicted to grow as $d\langle\lambda\rangle/dt = \langle\omega\rangle\langle\lambda\rangle$, and the average bubble height is $dh_B/dt = \langle u\rangle$, where $\langle\omega\rangle$ and $\langle u\rangle$ are the averages of the merger rate and the bubble velocity over the scale-invariant wavelength distribution. In the RT case, the model results in $h_B = \alpha_B g t^2$, where $\alpha_B = \langle u\rangle\langle\omega\rangle/(4g)$ [11,25]. Using the A dependence of $u \sim \sqrt{2A/(1 + A)}$ and $\omega \sim \sqrt{A(1 + A)/2}$ found above, we obtain the well-known experimental and numerical relation [4] $\alpha_B(A) = A\alpha_B(A = 1)$ [with $\alpha_B(A = 1) = 0.05$] [11]. In RM, $\langle\omega\rangle = t^{-1}\omega_0$ and $\langle u\rangle = c_B\lambda/t$ and hence $h_B(t) = a_B t^{\theta_B}$, where $\theta_B = \omega_0$. At $A = 1$ we find [11] $\omega_0 = 0.4$, and since the RM merger rate ω is found to be insensitive to A, we expect $\theta_B = \omega_0 \simeq 0.4$ at all A's. Note that the merger rate determines the power law in RM, while entering only in the coefficient α_B in RT. The coefficient a_B can be related to the initial conditions by considering the onset time of the scale-invariant regime $t_0 = \eta\tilde{\lambda}_0/\tilde{u}_0$, where $\tilde{\lambda}_0$ and $\tilde{u}_0$ are the average initial wavelength and velocity, and η, a parameter of order 1, depends on the initial spectrum. This yields $a_B = c_B/(\theta_B \eta^{\theta_B})\tilde{\lambda}_0^{1-\theta_B}\tilde{u}_0^{\theta_B}$ [using Richtmyer's formula [1] for $\tilde{u}_0$ yields $a_B \propto (A\Delta U)^{\theta_B}$, where ΔU is the interface jump velocity]. Hence, the bubble-front scaling law can be written as $h_B \sim \tilde{\lambda}_0(\tilde{u}_0 t/\tilde{\lambda}_0)^{\theta_B}$, showing that, in the absence of a length scale from a driving acceleration

(gt^2), the bubble-front height is composed of the length scales of the initial perturbation, $\tilde{u}_0 t$ and $\tilde{\lambda}_0$. To check these predictions, we performed simulations of multimode RM fronts at various A's. The initial perturbations in velocity were a sum of modes with wave numbers $k_l = \pi l/L$, with $l = 10$–40 and $L = 10$ cm and random amplitudes u_l such that $(\sum u_l^2)^{1/2} = 8$ cm/ms. Typically 200–300 zones were used in each direction, which is adequate for the bubbles but may somewhat underestimate the spike penetration. In Fig. 2, the bubble and spike penetrations are plotted versus $t^{0.4}$. After a short initial transient, the bubble and spike penetrations are both well fitted by power laws in time. In Fig. 2 inset, the power-law exponent θ is plotted for the bubbles and spikes. We find $\theta_B = 0.4 \pm 0.02$ for all A's in agreement with the theoretical prediction. Repeating the simulations, with all the wavelengths multiplied by a factor q of 2–100, it was found that $\theta_B = 0.4$ and $a_B \sim q^{0.6}$, in agreement with the predicted scaling. From Fig. 2, it is seen that the RM spike penetration is well fitted by $h_s = a_s t^{\theta_s}$, where θ_s goes from 1 at $A = 1$, where the spikes fall with a constant velocity, to $\theta_s = \theta_B \simeq 0.4$ at low Atwood numbers, where the bubble and spike fronts become symmetric. In the RT instability, the spike front grows as $h_s = \alpha_s g t^2$, where α_s/α_B is an increasing function of A [4,5]. The present model can help in understanding the spike-front evolution. The dominant spikes, generated by the dominant bubbles, exhibit roughly the same periodicity as the bubbles [25] [see Figs. 3(a) and 3(b)], and therefore can be described by the same merger rate ω. The dominant modes are not far from their saturation stage—the present model shows that in the scale invariant regime $h_B = b\langle\lambda\rangle$, with $b = c_B(A)/\omega_0 \approx 0.26 - 0.35$ in RM, and $b \approx 0.5/(1 + A)$ in RT. This suggests that the evolution equation for the spike front is $dh_s/dt = \langle u_s\rangle$, where u_s is the *spike velocity of a single mode when the bubble amplitude is* $b\lambda$, and the average is over the bubble-wavelength distribution. In RT, at $A \lesssim 0.5$ the single-mode spike velocity is already saturated when the bubble amplitude is $b\lambda$, and $\alpha_s/\alpha_B = u_s/u_B \approx \sqrt{(1 + A)/(1 - A)}$ [26], while at higher A's, the spike still accelerates at this stage, and α_s/α_B is lower than $\sqrt{(1 + A)/(1 - A)}$. The results for α_s/α_B, shown in Fig. 4(a), are in fair agreement with experimental and numerical data [4,5,26]. In RM, we find that the single-mode spike velocity (Fig. 1 inset) is $u_s \sim u_0(u_0 t/\lambda)^{-\beta}$, when the bubble amplitude is $b\lambda$. At low A's the spikes have already reached their asymptotic velocity ($\beta = 1$), while at higher A's they are still in a transient stage, and β decreases with A, reaching $\beta = 0$ at $A = 1$. This leads to $h_s \sim \tilde{\lambda}_0(\tilde{u}_0 t/\tilde{\lambda}_0)^{\theta_s}$, with $\theta_s = 1 - \beta(1 - \theta_B)$. The results for θ_s, shown in Fig. 4(b), tend to overestimate our simulation results at intermediate A's by about 20%.

In order to gain more insight into the model, we present in Fig. 3 an analysis of a multimode RM simulation. The early- and late-time interfaces, plotted in Figs. 3(a)

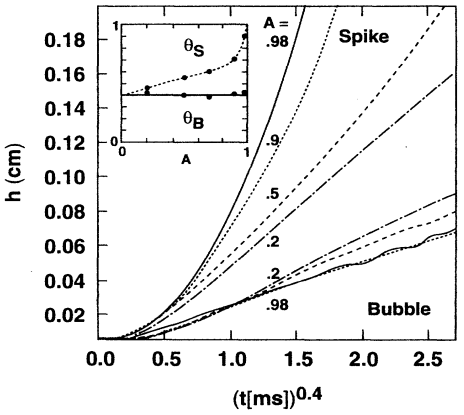

FIG. 2. RM random bubble- and spike-front penetration (defined at 90% of the heavy and light fluid volume fractions, respectively) versus $t^{0.4}$. Penetrations defined at higher volume fractions have the same θ and higher coefficients [see Fig. 3(e)], mainly for the spikes at high A (as in the RT case [4,5]). Inset: power-law exponent θ_B and θ_s.

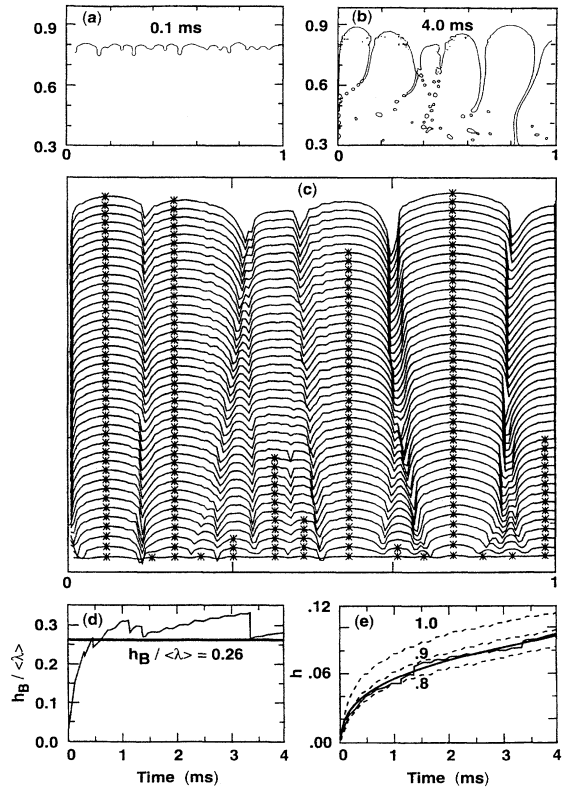

Fig. 3. Analysis of the $A = 0.98$ multimode RM simulation of Fig. 2. (a) Interface at $t = 1.0$ ms, and (b) $t = 4.0$ ms. (c) Bubble envelope (contour of maximum light fluid penetration), vertically offset by fixed intervals, at $t = 0.1$ ms and at equally spaced time intervals between $t = 1.0$ ms and $t = 4.0$ ms. Bubbles with a positive velocity are marked by *'s. (d) $b = h_B/\langle\lambda\rangle$, h_B is the average rising bubble height from simulation and model prediction $b = 0.26$. (e) h_B from simulation (line) and model (bold line) and penetration of 80%, 90%, and 100% heavy fluid volume fractions (dashed).

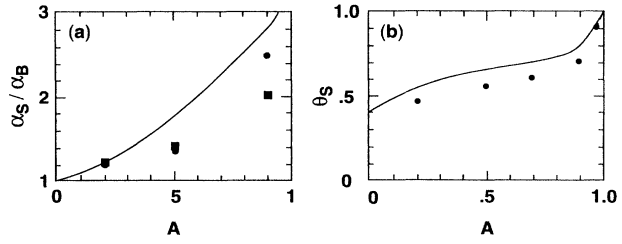

FIG. 4. (a) Model prediction for RT spike-front to bubble-front penetration ratio α_s/α_B (full line). ●'s, Youngs' simulations [4] and ■'s, Freed *et al.* simulations [5]. (b) Model prediction for RM spike front exponent θ_s (full line). ●'s present simulation results.

and 3(b), demonstrate the appearance of a large structure with similar bubble and spike periodicity. The bubble-competition process is illustrated in Fig. 3(c), showing the decreasing number of bubbles in the front. Since the front in the model consists of all rising bubbles [11], we define $\langle\lambda\rangle$ as the average wavelength of the bubbles with positive velocity (system size divided by the number of rising bubbles, in this case about $\frac{1}{2}$ of the bubbles) [27]. The ratio $h_B/\langle\lambda\rangle$ and the front height predicted by the model, using $dh_B/dt = (3\pi)^{-1}\langle\lambda\rangle/t$, are in good agreement with the simulation as shown in Figs. 3(d)–3(e), validating the main ingredients of the bubble-competition picture.

In conclusion, the bubble-competition picture can explain the RT scaling laws and predicts that the RM mixing zone grows as a sum of two different power laws and depends on the initial perturbation spectrum. Finally, we note that the present picture, in which the front evolution is controlled by the effect of drag on the large-scale structure, tends to support the assumptions of two-phase flow treatments of the instabilities [4,5] and may explain the difficulties encountered in may attempts to attribute the front evolution to the small scales, such as turbulent dissipation models [7].

We thank G. Hanoch, E. Waxman, C. P. Verdon, R. L. McCrory, S. W. Haan, M. Rosen, D. Mukamel, and I. Procaccia for helpful discussions. This work was partially supported by the U.S. Department of Energy Office of Inertial Confinement Fusion under Cooperative Agreement No. DE-FC03-92SF19460, the University of Rochester, and the New York State Energy Research and Development Authority.

[1] R. D. Richtmyer, Commun. Pure Appl. Math. **13**, 297 (1960); E. E. Meshkov, Fluid Dyn. **4**, 101 (1969).
[2] D. H. Sharp, Physica (Amsterdam) **12D**, 3 (1984).
[3] For a recent review, see J. D. Kilkenny *et al.*, Phys. Plasmas **1**, 1379 (1994).
[4] D. L. Youngs, Physica (Amsterdam) **12D**, 32 (1984); K. I. Read, Physica (Amsterdam) **12D**, 45 (1984).
[5] N. Freed, D. Ofer, D. Shvarts, and S. A. Orszag, Phys. Fluids A **3**, 912 (1991).
[6] A. N. Aleshin, E. V. Lazareva, S. G. Zaitsev, V. B. Rozanov, E. G. Gamalii, and I. G. Lebo, Sov. Phys. Dokl. **35**, 159 (1990); M. Brouillette and B. Sturtevant, Phys. Fluids A **5**, 916 (1993), and references therein.
[7] V. A. Andronov, S. M. Bakhrakh, E. E. Meshkov, V. V. Nikiforov, A. V. Pevnitskii, and A. I. Tolshmyakov, Sov. Phys. Dokl. **27**, 393 (1982); C. E. Leith, Lawrence Livermore National Laboratory Report No. UCRL-96036, 1986; S. Gauthier and M. Bonnet, Phys. Fluids A **2**, 1685 (1990).
[8] V. E. Neuvazhaev and I. E. Parshukov, Model. Mekh. **5**, 81 (1991).
[9] J. W. Grove, R. Holmes, D. H. Sharp, Y. Yang, and Q. Zhang, Phys. Rev. Lett. **71**, 3473 (1993).
[10] D. L. Youngs (to be published).
[11] U. Alon, J. Hecht, D. Mukamel, and D. Shvarts, Phys. Rev. Lett. **72**, 2867 (1994).
[12] D. Layzer, Astrophys. J. **122**, 1 (1955).
[13] J. Hecht, U. Alon, and D. Shvarts, Phys. Fluids **6**, 4019 (1994).
[14] C. L. Gardner, J. Glimm, O. McBryan, R. Menikoff, D. H. Sharp, and Q. Zhang, Phys. Fluids **31**, 447 (1988); J. Glimm, X. L. Li, R. Menikoff, D. H. Sharp, and Q. Zhang, Phys. Fluids A **2**, 2046 (1990).
[15] J. Glimm and D. H. Sharp, Phys. Rev. Lett. **64**, 2137 (1990); J. Glimm, Q. Zhang, and D. H. Sharp, Phys. Fluids A **3**, 1333 (1991).
[16] Y. Yang, Q. Zhang, and D. H. Sharp, Phys. Fluids **6**, 1856 (1994), and references therein.
[17] H. J. Kull, Phys. Rev. A **33**, 1957 (1986).
[18] S. W. Haan, Phys. Fluids B **3**, 2349 (1991).
[19] D. Ofer, D. Shvarts, Z. Zinamon, and S. A. Orszag, Phys. Fluids B **4**, 3549 (1992).
[20] H. Sakagami, A. V. Polionov, and K. Nishihara, in *Japan-U.S. Seminar on Physics of High Power Laser Matter Interactions,* edited by S. Nakai and G. H. Miley (World Scientific, Singapore, 1992), p. 361; V. I. Anisimov and A. V. Polionov, in *Proceedings of the 3rd International Conference on the Physics of Compressible Turbulent Mixing, Royaumont, France 1991* (World Scientific, Singapore, 1991), p. 299.
[21] At late times, Layzer's $A = 1$ model [12] reduces to this equation, with $V/S = \lambda$, $c_D = 3\pi$, and $c = \frac{1}{2}$. At $A < 1$, the inertia of the light fluid can be included on the left-hand side of the equation.
[22] H. Takabe and A. Yamamoto, Phys. Rev. A **44**, 5142 (1991).
[23] G. Birkhoff, in *Proceedings of Symposia in Applied Mathematics* (American Mathematical Society, Providence, 1962), Vol. XIII, p. 55; B. J. Daly, Phys. Fluids **10**, 297 (1967).
[24] J. A. Zufiria, Phys. Fluids **31**, 440 (1988).
[25] U. Alon, D. Shvarts, and D. Mukamel, Phys. Rev. E **48**, 1008 (1993).
[26] D. L. Youngs, in *Advances in Compressible Turbulent Mixing,* edited by W. P. Dannevik, A. C. Buckingham, and C. E. Leith (Princeton University, Princeton, New Jersey, 1992), p. 607, Conf-8810234.
[27] This definition of $\langle\lambda\rangle$ is qualitatively related to the enhancement of the single-bubble velocity by an envelope velocity used in the superposition hypothesis in Ref. [15]; D. H. Sharp (private communication).